

# Magnetic structures of $\text{PrMn}_2\text{Si}_2$ and $\text{NdMn}_2\text{Si}_2$ from neutron diffraction studies

R. Welter and G. Venturini

Laboratoire de Chimie du Solide Minéral, Associé au CNRS, UA 158, Université de Nancy I, BP 239, F-54506 Vandoeuvre Les Nancy Cédex (France)

D. Fruchart

Laboratoire de Cristallographie du CNRS, Associé à l'Université J. Fourier, 166 X, F-38042 Grenoble Cédex (France)

B. Malaman\*

Laboratoire de Chimie du Solide Minéral, Associé au CNRS, UA 158, Université de Nancy I, BP 239 F-54506 Vandoeuvre Les Nancy Cédex (France)

(Received August 31, 1992)

## Abstract

The magnetic properties of  $\text{PrMn}_2\text{Si}_2$  and  $\text{NdMn}_2\text{Si}_2$  have been reinvestigated. Below  $T_N$  (368 and 381 K for  $\text{PrMn}_2\text{Si}_2$  and  $\text{NdMn}_2\text{Si}_2$ , respectively) the previously proposed antiferromagnetic ordering taking place on the manganese sublattice is confirmed. Neutron diffraction experiments show that the Pr magnetic moments do not order above 1.6 K, while a ferromagnetic ordering of the neodymium sublattice occurs at  $T_C = 33(2)$  K ( $\mu_{\text{Nd}} = 2.83(4) \mu_B$  at 1.6 K). The magnetic coupling between the two sublattices is mainly ferromagnetic, with the easy axis of the magnetic structure aligned along the  $c$  axis, but a slight antiferromagnetic coupling remains between the Mn moments in the (001) plane ( $\mu_{\text{Mn}, F} = 1.4 \mu_B$  and  $\mu_{\text{Mn}, AF} = 0.8 \mu_B$  at 1.6 K).

## 1. Introduction

The ternary rare earth  $\text{RT}_2\text{X}_2$  compounds ( $R \equiv$  rare earth;  $T \equiv 3d, 4d$  or  $5d$  transition metal;  $X \equiv \text{Si, Ge}$ ) have been shown to exhibit very exciting physical properties ranging from superconductivity to heavy fermion behaviour [1, 2]. Most of them crystallize in the body centered tetragonal structure of the  $\text{ThCr}_2\text{Si}_2$  type (space group  $I4/mmm$ ) in which the rare earth and silicon atoms occupy the  $2(a)$  (0, 0, 0) and  $4(e)$  (0, 0,  $z$ ) (with  $z \approx 0.38$ ) sites respectively whereas the transition metal atom occupies the special position  $4(d)$  (0,  $\frac{1}{2}$ ,  $\frac{1}{4}$ ), *i.e.* with an additional  $C$  translation mode. The atoms are arranged in planes stacked perpendicular to the  $c$  axis in the sequence R–X–T–X–R (Fig. 1). The Si atoms form tetrahedra around the Mn atoms and the Mn–Si distances are very short, suggesting covalent bonding. These intermetallics usually order magnetically at low temperatures and present different types of magnetic structures. It has been reported that most of the compounds carry no magnetic moment on the T atom, while in  $\text{RMn}_2\text{X}_2$  compounds the Mn sublattice orders

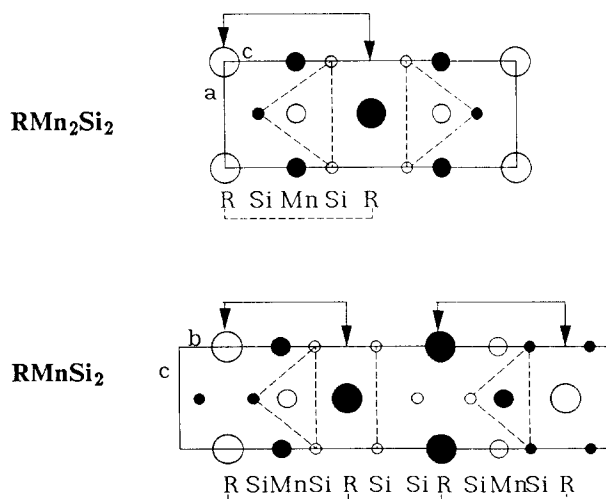


Fig. 1. Structural relationships of  $\text{RMn}_2\text{Si}_2$  ( $\text{ThCr}_2\text{Si}_2$  type) and  $\text{RMnSi}_2$  ( $\text{TbFeSi}_2$  type).

magnetically (ferromagnetically (F) or antiferromagnetically (AF); AF in the case of  $\text{RMn}_2\text{Si}_2$  except La) at relatively high temperatures (300–500 K). An additional magnetic transition, which corresponds to the

\*Author to whom correspondence should be addressed.

ordering of the R sublattice, generally occurs at low temperatures [2].

During the last decade the magnetic properties of the RMn<sub>2</sub>Si<sub>2</sub> compounds have been studied extensively by magnetometric and neutron diffraction techniques (see ref. 2, where a comprehensive review of the physical properties of these compounds can be found).

Nevertheless, the various studies devoted to NdMn<sub>2</sub>Si<sub>2</sub> and PrMn<sub>2</sub>Si<sub>2</sub> show some discrepancies. From magnetic measurements, Narasimhan *et al.* [33] concluded that NdMn<sub>2</sub>Si<sub>2</sub> and PrMn<sub>2</sub>Si<sub>2</sub> are antiferromagnetic below  $T_N = 380$  and 368 K respectively; below 36 K the Nd sublattice becomes ordered and ferromagnetically coupled with the Mn sublattice. Narasimhan *et al.* reported also that PrMn<sub>2</sub>Si<sub>2</sub> exhibits at 4.2 K a linear increase in magnetization as function of applied field. Later, from neutron diffraction experiments, Siek *et al.* [4] confirmed the high temperature antiferromagnetic structure of both compounds, but their neutron studies show that there is no magnetic order on the R sublattice at  $T > 1.8$  K. It has been suggested that the sudden drop in magnetization observed at low temperature might be the result of a metamagnetic transition. More recently a new magnetic measurement on NdMn<sub>2</sub>Si<sub>2</sub> has revealed the onset of ferromagnetism at 34 K under fields  $H > 0.4$  Oe [5], leading these authors to the same conclusion as Siek *et al.* [4]. Furthermore, Avdeev *et al.* [5] concluded that at  $H < 0.4$  Oe there is an additional antiferromagnetic phase.

On the other hand, our studies on the closely related PrMnSi<sub>2</sub> and NdMnSi<sub>2</sub> compounds [6, 7] have shown that magnetic ordering of the rare earth sublattices occurs below about 40 K. Accounting for the straight structural relationship exhibited by these two types of silicides, we restart a careful magnetic study of PrMn<sub>2</sub>Si<sub>2</sub> and NdMn<sub>2</sub>Si<sub>2</sub> using bulk magnetic measurements and neutron diffraction experiments.

## 2. Experimental procedures

The compounds were prepared from commercially available high purity elements. Pellets of stoichiometric mixture were compacted using a steel die and then introduced into silica tubes sealed under argon (100 mmHg). The samples were first heated at 1073 K for preliminary homogenization treatment and then melted in an induction furnace. The resulting ingots were annealed for 5 days at 1273 K and finally quenched in water. The purity of the final samples was checked by the powder X-ray diffraction technique (Guinier camera and curved detector INEL CPS 120, Cu K $\alpha$  radiation).

The magnetic measurements were carried out on a Faraday balance (above 300 K) or on a Foner mag-

netometer (between 4.2 and 300 K) in fields up to 2 T.

Neutron diffraction experiments were carried out at the Institut Laue-Langevin (ILL), Grenoble. The diffraction patterns were recorded with the one-dimensional curved multidetector D1b at a wavelength  $\lambda = 2.5232$  Å. Several patterns were collected in the temperature range 1.6–300 K. No pattern was collected in the paramagnetic state ( $T_N > 370$  K). The first refinements pointed to the occurrence of texture effects (owing to tablet-like crystallites, the  $c$  axis takes a preferential orientation perpendicular to the neutron beam). In order to correct this effect, we followed the suggestion of Dollase [8] and used the March formula [9]

$$M_{hkl} = \left( f_{\text{cor}} \cos^2 \alpha + \frac{\sin^2 \alpha}{f_{\text{cor}}} \right)^{-3/2}$$

where  $M_{hkl}$  is a corrective factor for the calculated intensity of each line,  $f_{\text{cor}}$  is a fitted coefficient which reflects the degree of preferential orientation and  $\alpha$  is the angle between the  $c$  axis and the  $hkl$  plane in the Bragg position. The value of  $f_{\text{cor}}$  obtained for refinements of each compound (see Section 3.2.1 and Table 2) strongly supports the validity of this correction. Using the Fermi lengths tabulated by Sears [10] and the magnetic form factors of Mn and R<sup>3+</sup> taken from ref. 11, the scaling factor  $f_{\text{cor}}$ , the atomic position  $z_{\text{Si}}$  and the magnetic moments of Mn and R<sup>3+</sup> were refined by the MXD least-squares fit procedure [12]. The MXD programme allows simultaneous fitting of the nuclear and magnetic intensities to the observed ones.

In every case attempts to fit the nuclear lines by interchanging the positions of the Mn and Si atoms always led to a poorer agreement and gave no evidence for any mixing between the Mn and Si atoms at 4( $d$ ) and 4( $e$ ) sites as observed by Siek *et al.* [4].

Moreover, it is important to stress that the Mn sublattice has also a  $C$  lattice mode (see Section 1). Thus the magnetic contributions to the observed intensities due to ferromagnetic ordering of the Mn atoms affect only the nuclear lines obeying the condition limiting possible reflections: ( $hkl$ ) with  $h + k = 2n$ .

## 3. Experimental results

X-ray diffraction analysis confirmed that both samples prepared were single phases with the crystal structure of the ThCr<sub>2</sub>Si<sub>2</sub> type. The lattice parameters at room temperature of PrMn<sub>2</sub>Si<sub>2</sub> ( $a = 4.027(3)$  Å,  $c = 10.563(5)$  Å) and NdMn<sub>2</sub>Si<sub>2</sub> ( $a = 4.013(3)$  Å,  $c = 10.554(5)$  Å) are in good agreement with the previously published values [13].

TABLE 1. RMn<sub>2</sub>Si<sub>2</sub> and RMnSi<sub>2</sub> [6] (R ≡ Pr, Nd) magnetic data

Compounds	$T_i \pm 2$ (K)		$\theta_P$ (K)	$\mu_{\text{eff}}$ ( $\mu_B$ )	$\mu_{\text{th}}(\text{R}^{3+})$ ( $\mu_B$ )	$\mu_{\text{eff}}(\text{Mn})$ ( $\mu_B$ )	$H_C(4.2 \text{ K})$ (kG)	$M(4.2 \text{ K}, 2 \text{ T})$ ( $\mu_B$ )
	$T_N$	$T_C$						
PrMn <sub>2</sub> Si <sub>2</sub>	368	–	275	5.3	3.58	~2.8	–	–
NdMn <sub>2</sub> Si <sub>2</sub>	382	34	287	5.4	3.62	~2.9	1.4	4.16
PrMnSi <sub>2</sub> <sup>a</sup>	35–434	–	450	4.29	3.58	~2.6	4 <sup>b</sup>	4.00
NdMnSi <sub>2</sub>	441	40	460	4.41	3.62	~2.6	3.5 <sup>b</sup>	4.10

<sup>a</sup>Metamagnetic transition at 28 kG; <sup>b</sup>at 77 K.

### 3.1. Susceptibility measurements

The main characteristic magnetic data are collected in Table 1.

PrMn<sub>2</sub>Si<sub>2</sub> and NdMn<sub>2</sub>Si<sub>2</sub> order antiferromagnetically at  $T_N = 368$  and  $381$  K respectively. In both cases the reciprocal susceptibility obeys the Curie–Weiss law at high temperatures. The positive paramagnetic Curie temperatures  $\theta_P$  (Table 1) indicate that the interactions have mainly a ferromagnetic character in these two compounds. The Mn paramagnetic moments have been calculated assuming the theoretical free-ion value for the rare earth element R. It may be noted that the values so obtained are close to those observed in the corresponding RMnSi<sub>2</sub> compounds (Table 1).

No further magnetic transition is observed for PrMn<sub>2</sub>Si<sub>2</sub> above 4.2 K, whereas NdMn<sub>2</sub>Si<sub>2</sub> shows a large increase in its susceptibility at  $T_i = 33(2)$  K (see inset in Fig. 2). The magnetization curves recorded at 4.2 K (Fig. 3) indicate a ferromagnetic behaviour with a magnetization moment value of  $4.16(5) \mu_B$  per formula unit (f.u.) at 20 kG. Moreover, NdMn<sub>2</sub>Si<sub>2</sub> displays a substantial coercive field ( $H_C \approx 1.4$  kG, Fig. 3), which points to a strong uniaxial anisotropy in this material in agreement with the particular aspect of its thermomagnetic curve (Fig. 2).

All these results are in good agreement with those reported in refs. 3–5. Moreover, Table 1 compares the magnetic parameters obtained for PrMn<sub>2</sub>Si<sub>2</sub> and

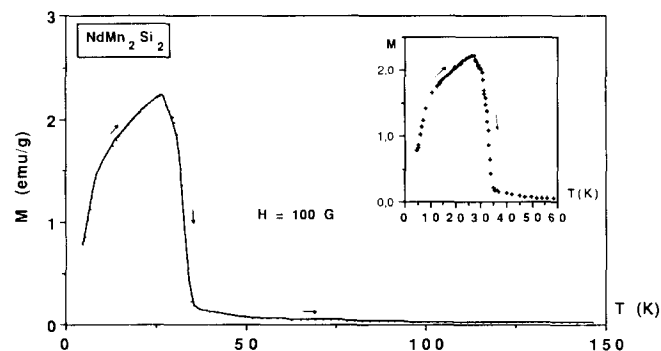


Fig. 2. Temperature dependence of magnetization in NdMn<sub>2</sub>Si<sub>2</sub> measured at  $H = 100$  G.

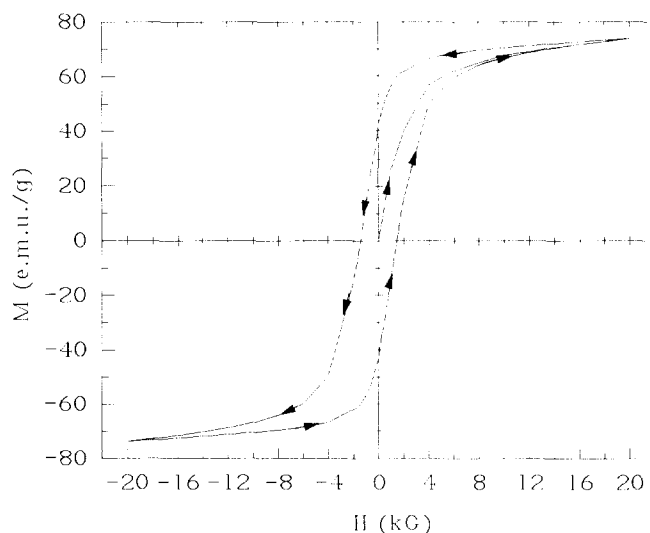


Fig. 3. Hysteresis loop at 4.2 K in NdMn<sub>2</sub>Si<sub>2</sub>.

NdMn<sub>2</sub>Si<sub>2</sub> with those observed for the corresponding RMnSi<sub>2</sub> compounds [6].

### 3.2. Neutron diffraction studies

#### 3.2.1. PrMn<sub>2</sub>Si<sub>2</sub>

For PrMn<sub>2</sub>Si<sub>2</sub> the neutron diffraction patterns are similar over the whole temperature range studied (1.6–300 K). According to ref. 4, this result confirms the magnetometric data showing that magnetic moments of the Pr sublattice did not order at low temperature. All the reflections observed on the neutron diffraction patterns (Fig. 4) can be easily indexed on the basis of the crystallographic unit cell. Three superlattice lines of magnetic origin can be identified (the remaining lines are characteristic of only nuclear scattering with no magnetic contributions). They are indexed as (111), (113) and (201) with the following extinction rules for  $hkl$ :  $h+k+l=2n$  and  $h+k=2n+1$ , corresponding to the magnetic antitranlation mode  $I'$  and the  $C$  translation mode respectively. This suggests a simple antiferromagnetic structure based on the stacking of ferromagnetic (001) Mn planes in a  $+ - + -$  sequence along the  $c$  axis. The absence of the (00 $l$ ) peaks can be attributed to the geometrical term of the magnetic

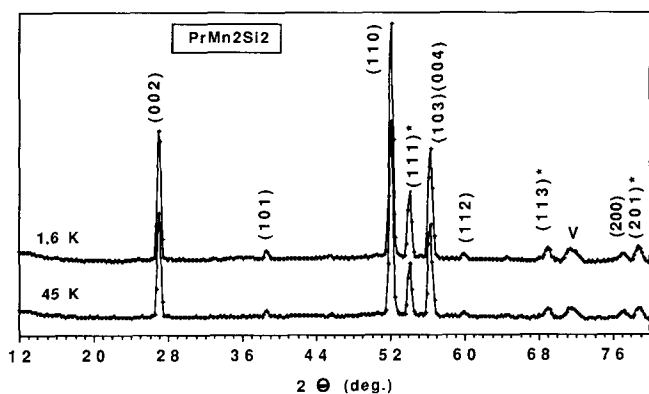


Fig. 4. Neutron diffraction patterns of  $\text{PrMn}_2\text{Si}_2$  at 45 and 1.6 K.

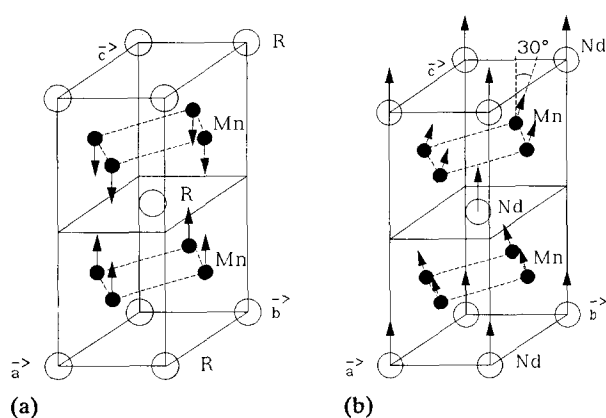


Fig. 5. (a) Magnetic structure of  $\text{PrMn}_2\text{Si}_2$  (magnetic structure of  $\text{NdMn}_2\text{Si}_2$  at high temperature). (b) Magnetic structure of  $\text{NdMn}_2\text{Si}_2$  at 1.6 K.

structure factor and leads to alignment of the Mn moments along the  $c$  axis. This type of magnetic ordering is usually referred to as type AFI [2] and is shown in Fig. 5.

The refined parameters are collected in Table 2 together with the observed and calculated intensities. At 1.6 K the magnetic moment of Mn atoms is  $2.03(2) \mu_B$ . This value is a little smaller than that obtained by Siek *et al.* ( $2.45 \mu_B$ ) [4] (probably owing to the fact that those authors did not correct the texture effects).

### 3.2.2. $\text{NdMn}_2\text{Si}_2$

The temperature dependence of the neutron diffraction patterns recorded stepwise from room temperature to 1.6 K leads to the following conclusions.

(1) Between 300 K and  $T_1 \approx 33$  K the patterns (Fig. 6) are quite similar to those observed for  $\text{PrMn}_2\text{Si}_2$ , yielding the same antiferromagnetic ordering on the Mn sublattice (Fig. 5). The refined parameters are collected in Table 2 together with the observed and calculated intensities. At 45 K the magnetic moment of the Mn atoms is  $1.92(3) \mu_B$  (*vs.*  $2.5 \mu_B$  obtained by Siek *et al.* [4]; see Section 3.2.1.).

(2) Below 33 K a strong decrease in the intensities of the previous magnetic lines and an increase in all the intensities of the nuclear peaks (except for the  $(00l)$  lines) are observed. This implies that a ferromagnetic ordering occurs on decreasing the temperature, in agreement with the magnetometric measurements. Simultaneously, new magnetic lines which can be indexed as  $(001)$  and  $(003)$  appear (Fig. 6). Contrary to the results of Siek *et al.* [4], evidence of ferromagnetic ordering of the neodymium sublattice is clearly obtained from the growth of the  $(101)$  peak, since, owing to the special position of manganese atoms (see Section 2), ferromagnetic ordering of the Mn sublattice cannot contribute to this peak. Moreover, the existence of the  $(00l)$  lines with  $l=2n+1$  can be attributed unambiguously to some deviation from the  $c$  axis of the Mn moment direction (in agreement with the magnetic antitranslation  $I'$ ), since the absence of the  $(h0l)$  peaks with  $h=2n+1$  (Fig. 6) indicates a magnetic  $C$  translation mode.

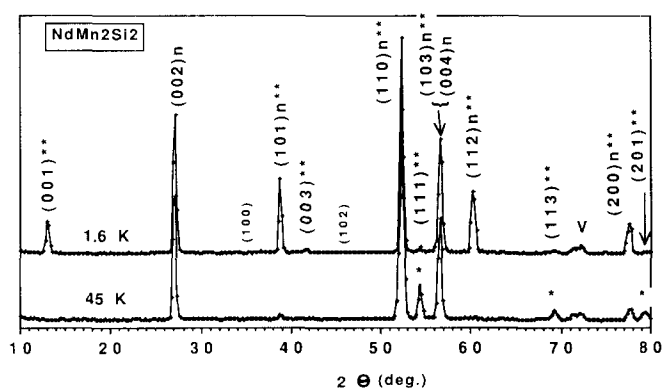
From these observations refinements were performed to account for the following magnetic model: a canted ferromagnetic structure in which the neodymium moments lie along the  $c$  axis; the manganese moments are parallel to each other in their own layers and are canted between the Mn sublayers. The antiferromagnetic component of the Mn moments lies in the  $(001)$  plane, whereas the ferromagnetic component is parallel to the Nd moment (Fig. 5).

The final refinement leads to a residual factor  $R=1.06\%$ . Table 2 gives the observed and calculated intensities and also the adjustable parameters ( $z_{\text{Si}}$ ,  $\mu_{\text{Mn}}$  and  $\mu_{\text{Nd}}$ ). At 1.6 K the canting angle of the Mn moment from the  $c$  axis is  $\alpha=30(1)^\circ$ . The Mn magnetic moment is found to be  $\mu_{\text{Mn}}=1.61(5) \mu_B$ , a value which is a little smaller than that observed at higher temperature. For the Nd atom a moment value  $\mu_{\text{Nd}}=2.83(4) \mu_B$  ( $gJ=3.20 \mu_B$ ) is obtained, indicating that the neodymium moment is slightly quenched by the crystalline electric field (CEF) effect. These values imply a total resulting moment of about  $5.6 \mu_B$  per formula unit, which is a higher value than that obtained by magnetization measurements (Table 1).

The thermal dependence of the  $(101)$  magnetic peak intensity (Fig. 7) gives an Nd sublattice ordering temperature  $T_C=(34 \pm 3)$  K, in fair agreement with the magnetic measurements (Table 1 [3–5]). Moreover, it is worth noting that whereas the magnetization curve reported in Fig. 2 gives evidence of a fast increase in the signal at about 34 K, the neutron diffraction experiments show (accounting for the behaviour of the  $(001)$ ,  $(111)$  and  $(112)$  peak intensities in Fig. 7) that a rather smooth Mn magnetic moment reorientation process takes place below  $T_C$ . Finally, it should also be noted that the variation in the intensities of all

TABLE 2. Lattice parameters,  $c/a$  ratio, atomic position  $z_{\text{Si}}$ ,  $f_{\text{cor}}$ , calculated and observed intensities, magnetic moments and reliability factors at 45 and 1.6 K for PrMn<sub>2</sub>Si<sub>2</sub> and NdMn<sub>2</sub>Si<sub>2</sub>

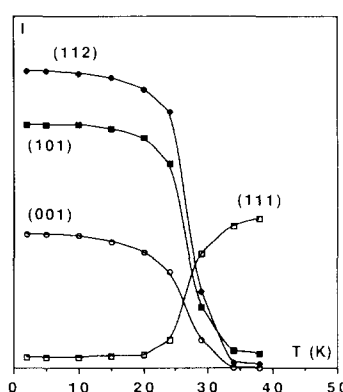
	PrMn <sub>2</sub> Si <sub>2</sub>				NdMn <sub>2</sub> Si <sub>2</sub>			
	$T=45$ K		$T=1.6$ K		$T=45$ K		$T=1.6$ K	
$a$ (Å)	4.020(3)		4.019(3)		3.998(3)		3.996(3)	
$c$ (Å)	10.548(7)		10.551(7)		10.510(7)		10.478(7)	
$c/a$	2.624		2.625		2.629		2.622	
$z_{\text{Si}}$	0.3799(7)		0.3807(5)		0.3806(6)		0.3797(5)	
$f_{\text{cor}}$	1.067(5)		1.058(4)		1.048(3)		1.052(5)	
$hkl$	$I_o$	$I_c$	$I_o$	$I_c$	$I_o$	$I_c$	$I_o$	$I_c$
001	–	–	–	–	–	–	7	7
002	109	109	136	136	95	95	94	94
100	–	–	–	–	–	–	0	0
101	12	10	16	12	6	5	94	93
003	–	–	–	–	–	–	5	5
102	–	–	–	–	–	–	0	0
110	773	774	916	918	520	519	538	535
111	203	201	262	261	97	97	10	10
004	–	–	–	–	–	–	–	–
103	408	406	484	483	305	305	352	352
112	17	22	25	24	3	2	215	211
104	–	–	–	–	–	–	–	–
113	78	85	107	112	45	42	12	8
200	70	54	80	64	59	70	166	186
201	111	120	153	156	54	58	5	5
$\mu_{\text{Mn}}$ ( $\mu_{\text{B}}$ )	1.94(3)		2.03(2)		1.92(3)		1.61(5)	
	$c$		$c$		$c$		$\alpha=30(1)^\circ$	
$\mu_{\text{R}}$ ( $\mu_{\text{B}}$ )	–		–		–		2.83(4)	
	–		–		–		$c$	
$R$ (%)	1.70		1.47		1.50		1.06	

Fig. 6. Neutron diffraction patterns of NdMn<sub>2</sub>Si<sub>2</sub> at 1.6 and 45 K.

these peaks begins at the same time. This implies that the low temperature magnetic ordering takes place simultaneously on both the Nd and Mn sublattices.

#### 4. Discussion

The main result provided by this study is the evidence of a low temperature ferromagnetic ordering on the

Fig. 7. NdMn<sub>2</sub>Si<sub>2</sub>: temperature dependence of integrated intensities of (001) (101), (111) and (112) lines.

Nd sublattice — in good agreement with previous conclusions of Narasimhan *et al.* [3] — as observed in other members of the RMn<sub>2</sub>Si<sub>2</sub> series (R ≡ Gd–Dy, Er) [2]. This behaviour implies that the interlayer R–R interactions are positive and relatively strong with respect to the rather high transition temperatures observed

in this series. It should be noted that under these conditions the  $\text{RMn}_2\text{Si}_2$  compounds differ from the other  $\text{ThCr}_2\text{Si}_2$ -type structure  $\text{RT}_2\text{X}_2$  compounds ( $\text{T} \equiv \text{Fe-Cu}$ ;  $\text{X} \equiv \text{Si, Ge}$  [2]) where the rare earth sublattices are antiferromagnetically ordered even though the R–R nearest interlayer interactions (Fig. 1) are ferromagnetic. These differences may be explained if one takes into account the fact that in all these compounds the prevailing magnetic interactions are of the Ruderman–Kittel–Kasuya–Yasuda (RKKY) type and thus depend on the number of conduction electrons ( $T$ ) and on the R–R distance ( $c/a$  ratio).

The second remark relates to the R–Mn couplings. In the case of  $\text{NdMn}_2\text{Si}_2$  the R magnetic ordering yields a spin reorientation phenomenon. Iwata *et al.* [14] have shown that for light rare earths the ferromagnetic coupling between the R and Mn sublattices is dominant. Therefore this interaction allows us to stabilize in  $\text{NdMn}_2\text{Si}_2$  a ferromagnetic structure below 33 K. The Mn–Mn interlayer interaction is antiferromagnetic as deduced from the high temperature magnetic structure. Since the R magnetic system is the most strictly governed by magnetocrystalline anisotropy (CEF), the spin rotation process concerns the Mn sublattice at  $T_{\text{SR}} = 33$  K, when the positive Nd–Mn interactions counterbalance the negative Mn–Mn ones. The shortest Mn–Mn interaction distances,  $d_{\text{Mn-Mn}}(c/2) = 5.25 \text{ \AA}$ , are four times less numerous than the shortest Mn–Nd distances,  $d_{\text{Mn-Nd}}([(a/2)^2 + (c/4)^2]^{1/2}) = 3.3 \text{ \AA}$  (Fig. 5), and accounting for the respective magnetic moments measured apart from  $T_{\text{SR}}$ , the ratio  $T_{\text{N}}/T_{\text{SR}} \approx 11.5$  has a reasonable magnitude.

However, the reorientation of the Mn moment is not complete and a partial antiferromagnetic ordering between each Mn (001) plane remains down to 1.6 K. It results in a canted ferromagnetic ordering on the Mn sublattice with a deviation of the moments from the easy axis of  $\alpha \approx 30^\circ$  at 1.6 K. The same behaviour is also encountered with the heavy rare earth  $\text{TbMn}_2\text{Si}_2$  compound, where, according to the dominant antiferromagnetic R–Mn coupling [14], a canted ferrimagnetic structure is observed [15]. This frustrated behaviour of the Mn moment could explain the slight reduction observed at 1.6 K ( $1.6 \mu_{\text{B}}$ ) from the 45 K value ( $1.9 \mu_{\text{B}}$ ) ( $1.8 \mu_{\text{B}}$  in  $\text{TbMn}_2\text{Si}_2$  at 4.2 K) and reflects the relative strength of the R–R, Mn–Mn and R–Mn interactions. On the other hand, the Nd moment value is close to the theoretical one. The discrepancy between the resulting magnetization measured at 2 T and that of the moments deduced from neutron diffraction shows that saturation is not reached under this field. In a powder sample it can be due either to a statistical distribution of the easy magnetization axis, which is characteristic of a rather strong anisotropy, or to more or less complex domain wall propagation as revealed

by the rather high coercive field ( $H_{\text{C}} \approx 1.4 \text{ kG}$ ). Finally, it is important to note that the canted ferromagnetic structure of  $\text{NdMn}_2\text{Si}_2$  at low temperature explains well the magnetization data obtained by Aldeev *et al.* [5] in very weak external fields (see Section 1).

One of the remaining questions concerns the pertinent parameters involved in the spin reorientation process and whether it is of second or first order. The magnetization curve reported in Fig. 2 shows a fast increase in the signal between 34 to 28 K. However, the magnetization decrease then observed could be the result of the limited applied field in comparison with the increasing critical field of a metamagnetic process (*e.g.*  $\text{PrMnSi}_2$  [6], Table 1). Low and high field magnetic measurements on single crystals are highly desirable for a better understanding of this point. By the way, neutron diffraction experiments show a rather smooth phenomenon to take place, accounting for the intensity behaviour of some peaks (Fig. 7).

In previous papers [7, 16] we have emphasized the structural relationships between the  $\text{ThCr}_2\text{Si}_2$ - and  $\text{TbFeSi}_2$ -type structures:  $\text{TbFeSi}_2$  could be described as isolated  $\text{ThCr}_2\text{Si}_2$ -type blocks (including Fe atoms) connected by Si–Si slabs (Fig. 1). It could be assumed that such structural relationships would lead to similar magnetic behaviours. An extensive comparison of the magnetic properties of the  $\text{RMn}_2\text{Si}_2$  and  $\text{RMnSi}_2$  compounds has been made in a previous paper [7] and it is of interest to remark that  $\text{NdMn}_2\text{Si}_2$  and  $\text{NdMnSi}_2$  have similar magnetic structures and that an Mn moment reorientation process is also encountered in the latter phase below 40 K [7]. In the structure-related silicides  $\text{NdMn}_2\text{Si}_2$  and  $\text{NdMnSi}_2$  the Mn environment is the same (Fig. 1). Comparable ways of describing the exchange interactions acting between the Mn and Nd sublattices can be found. Since the onset of the rare earth magnetic ordering in  $\text{RMnSi}_2$  [7] has led to the discovery of a similar phenomenon occurring in the parent compound  $\text{NdMn}_2\text{Si}_2$ , it may be assumed that the exchange interactions are of a similar nature and comparable in strength.

For  $\text{PrMn}_2\text{Si}_2$  the situation could be more complicated in terms of exchange couplings. In fact, in  $\text{PrMnSi}_2$  [7] we have shown that the magnetic interactions acting between Pr and Mn are strongly negative at short distances ( $d_1$ ) (forcing the ferromagnetically coupled Mn sublattice to rotate at  $T_{\text{SR}} = 34$  K) but are positive for next-nearest neighbours ( $d_2$  and  $d_3$ , Fig. 1) (see also Fig. 5 of ref. 7). Furthermore, we have previously noticed (see above) that in most  $\text{RT}_2\text{X}_2$  compounds the R–R next-nearest-neighbour interactions are negative. Therefore in  $\text{PrMn}_2\text{Si}_2$  all such interactions would lead to a frustrated behaviour of the Pr sublattice and could explain the absence of Pr ordering. A more detailed review of competing interactions acting on the

moments in such layered structures can be found in refs. 7, 16 and 17.

On the other hand, the values of the magnetic moments measured at 1.6 K are similar to those observed in the corresponding RT<sub>2</sub>Si<sub>2</sub> compounds. They are close to the theoretical values for the heavy rare earths and slightly reduced for the Nd compound. However, it is worth noting that a large reduction of the Pr moment is observed in PrFe<sub>2</sub>Si<sub>2</sub> (1.45  $\mu_B$  vs. about 2.8  $\mu_B$  in PrFe<sub>2</sub>Ge<sub>2</sub> and NdFe<sub>2</sub>Si<sub>2</sub>) [18], with an ordering temperature of 6 K vs. 13 and 16 K for NdFe<sub>2</sub>Si<sub>2</sub> and PrFe<sub>2</sub>Ge<sub>2</sub> respectively). This result can be explained in the frame of a crystal field model which shows that the magnetic moment value depends critically on the higher order CEF parameters, particularly on  $B_4^4$  [18]. A still more important reduction of the moment in PrMn<sub>2</sub>Si<sub>2</sub> might perhaps explain the lack of ordering of the Pr sublattice above 1.6 K in this compound. The possibility that, owing to the crystal field splitting, the lowest level is a non-magnetic singlet level might also explain the lack of ordering of the Pr sublattice.

In order to obtain more detailed information regarding this point and to reach a better understanding of the magnetic behaviour of this kind of compound, further low temperature neutron investigations on PrMn<sub>2</sub>Ge<sub>2</sub> and NdMn<sub>2</sub>Ge<sub>2</sub> compounds are in progress.

## 5. Conclusions

The determination of the magnetic properties of RMn<sub>2</sub>Si<sub>2</sub> (R  $\equiv$  Pr, Nd) compounds gives new information on the magnetic interactions in rare earth ternary iron silicides of the ThCr<sub>2</sub>Si<sub>2</sub>-type structure and allows us to make some comparisons with the closely related RMnSi<sub>2</sub>.

Our neutron diffraction study indicates that PrMn<sub>2</sub>Si<sub>2</sub> and NdMn<sub>2</sub>Si<sub>2</sub> exhibit antiferromagnetic ordering of the Mn sublattice below  $T_N = 365$  and 381 K respectively with an Mn moment of about 2  $\mu_B$ . The intralayer ((001) planes) ordering of Mn moments is ferromagnetic because of the strong ferromagnetic intralayer interactions which are responsible for the high paramagnetic Curie temperature.

No magnetic ordering occurs in PrMn<sub>2</sub>Si<sub>2</sub> above 1.6 K, while NdMn<sub>2</sub>Si<sub>2</sub> exhibits ferromagnetic ordering of the Nd sublattice at 33 K. The positive Nd–Mn interactions imply a spin reorientation process on the Mn sublattice yielding a canted ferromagnetic structure at 1.6 K. In addition, NdMn<sub>2</sub>Si<sub>2</sub> presents high coercive field (about 1.4 kG at 4.2 K), attesting a strong uniaxial anisotropy.

The orientation of the R moments with respect to the crystal [001] axis is probably determined by the

sign of  $A_2^0$ . In the case of NdMn<sub>2</sub>Si<sub>2</sub> a [001] easy axis direction indicates that  $A_2^0$  should be positive [7, 16–20]. The influence of crystal field effects may also explain the partial quenching of the Nd moment, which is somewhat smaller than the R free-ion value, and the absence of magnetic ordering in PrMn<sub>2</sub>Si<sub>2</sub>.

The magnetic properties are very similar to those found in most of the corresponding ThCr<sub>2</sub>Si<sub>2</sub>- and TbFeSi<sub>2</sub>-type structure compounds, in agreement with the underlying structural relationships. In all these compounds the long-range magnetic ordering along the stacking axis depends on interactions of the RKKY type and is characteristic of a layer structure with competing coupling tendencies.

## Acknowledgments

We are indebted to the Institut Laue–Langevin (Grenoble) for the provision of research facilities. Magnetic measurements were undertaken at the Service Commun de Magnétométrie de l'Université de Nancy I. We are grateful to Dr. J. Hubsch, responsible for the magnetometer used, and Dr. J. L. Soubeyrou, responsible for the Dlb spectrometer, for their help during the measurements.

## References

- 1 H. R. Ott and Z. Fisk, in A. J. Freeman and G. H. Lander (eds.), *Handbook on the Physics and Chemistry of the Actinides*, Vol. 5, North-Holland, Amsterdam, 1987, p. 85.
- 2 A. Szytula and J. Leciejewicz, in K. A. Gscheidner Jr. and L. Eyring (eds.), *Handbook on the Physics and Chemistry of Rare Earths*, Vol. 12, Elsevier, New York, 1989, p. 133.
- 3 K. S. V. L. Narasimhan, V. U. S. Rao, W. E. Wallace and I. Pop, *AIP Conf. Proc.*, 29 (1975) 594.
- 4 S. Siek, A. Szytula and J. Leciejewicz, *Solid State Commun.*, 39 (1981) 863.
- 5 L. Z. Avdeev, S. A. Nikitin, O. V. Snigirev, A. M. Tishin and V. V. Khanin, *Sov. Phys. – Solid State*, 30(2) (1988) 339.
- 6 G. Venturini, B. Malaman, M. Meot-Meyer, D. Fruchart, G. Le Caer, D. Malterre and B. Roques, *Rev. Chim. Minér.*, 23 (1986) 162.
- 7 B. Malaman, G. Venturini, L. Pontonnier and D. Fruchart, *J. Magn. Magn. Mater.*, 86 (1990) 349.
- 8 W. A. Dollase, *J. Appl. Crystallogr.*, 19 (1986) 267.
- 9 A. March, *Z. Kristallogr.*, 81 (1932) 285.
- 10 V. F. Sears, *Internal Rep. AECL-8490*, 1984 (Chalk River Nuclear Laboratories).
- 11 A. J. Freeman and J. P. Declaux, *J. Magn. Magn. Mater.*, 69 (1979) 61.
- 12 C. G. Shull and Y. Yamada, *J. Phys. Soc. Jpn.*, 22 (1962) 1210.
- 12 P. Wolfers, *J. Appl. Crystallogr.*, 23 (1990) 554.

- 13 D. Rossi, R. Mazzara, D. Mazzone and R. Ferro, *J. Less-Common Met.*, 59 (1978) 79.
- 14 N. Iwata, T. Ikeda, T. Shigeoka, H. Fujii and T. J. Okamoto, *J. Magn. Magn. Mater.*, 54–57 (1985) 481.
- 15 T. Shigeoka, N. Iwata, H. Fujii and T. J. Okamoto, *J. Magn. Magn. Mater.*, 63–64 (1986) 1343.
- 16 B. Malaman, G. Venturini, L. Pontonnier, D. Fruchart, G. Le Caer, K. Tomala and J. P. Sanchez, *Phys. Rev.*, 41(7) (1990) 4700.
- 17 R. Welter, G. Venturini and B. Malaman, *J. Alloys Comp.*, 189 (1992) 49.
- 18 B. Malaman, G. Venturini, A. Blaise, J. P. Sanchez and G. Amoretti, *Phys. Rev.*, in press.
- 19 W. E. Wallace, *Rare Earth Intermetallic* Academic, New York, 1973, Chap. 3.
- 20 J. E. Greedan and V. U. S. Rao, *J. Solid State Chem.*, 6 (1973) 387.